Acknowledgment. The support of the National Science Foundation, the donors of the Petroleum Research Fund, administered by the American Chemical Society, and the U.S. Air Force Geophysical Laboratory is gratefully acknowledged. We also acknowledge with thanks the kindness of Professor J. H. Futrell in providing the use of the tandem ICR instrument at Utah and in supporting R.G.O.'s work on it.

Registry No. Allyl chloride radical cation, 82880-45-3; *cis*-1-chloropropene radical cation, 82916-36-7; *trans*-1-chloropropene radical cation, 82916-37-8; vinyl chloride radical cation, 50910-56-0; 2-chloropropene radical cation, 82880-46-4; propene radical cation, 34504-10-4; 1-chloropropane, 540-54-5; 2-chloropropane, 75-29-6.

Nucleophilic Attack and Structural Rearrangements in Some Iron Carbonyl Cluster Carbides. Syntheses, Structures, and Reactions of the Tetrahedral Four-Iron Clusters $[Fe_4(CO)_{12}(\mu_3\text{-}COCH_3)]^-$ and $[Fe_4(CO)_{12}(CCH_3)]^-$

E. M. Holt,*[1a] K. H. Whitmire,[1b] and D. F. Shriver*[1b]

Contribution from the Departments of Chemistry, Northwestern University, Evanston, Illinois 60201, and Oklahoma State University, Stillwater, Oklahoma 74078.
Received January 19, 1982

Abstract: The reaction of the four-iron butterfly compound $[Fe_4(CO)_{12}C]^{2-}$ with the strong carbocation reagent $CH_3SO_3CF_3$ leads to alkylation of the carbide carbon and structural rearrangement of the metal framework to produce a tetrahedral ethyne compound, $[Fe_4(CO)_{12}(\mu_3\text{-}CCH_3)]^-$. The rearrangement is readily explained by the cluster valence electron count. The tetrahedral carbonyl anion $[Fe_4(CO)_{12}(\mu_3\text{-}CO)]^{2-}$ in the presence of $CH_3SO_3CF_3$ is alkylated on the oxygen of a trihapto carbonyl to produce $[Fe_4(CO)_{12}(\mu_3\text{-}COCH_3)]^-$, in which the tetrahedral iron array is retained. In this case, alkylation does not change the formal count of electrons available for cluster bonding and therefore does not change the geometry of the four-iron array. There is, however, an inductive electron demand imposed on the cluster by O-alkylation, and this appears to be responsible for the shift of ancillary semibridging CO ligands into terminal positions.

The four-iron carbonyl cluster compounds such as $[Fe_4(CO)_{12}(\mu_3\text{-}CO)]^{2-}$ (I) display novel chemistry and structural transformations. The first indication of this unusual chemistry was the discovery that protonation of I leads to a rearrangement of the four-iron skeleton from a tetrahedral to a butterfly array (eq 1).[2] More recently, four-iron butterfly carbides have been

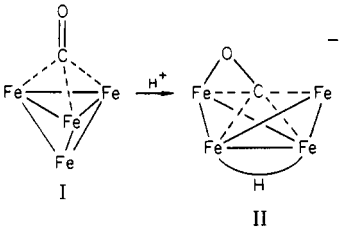

I II (1)

Fe = iron with three attached CO ligands

discovered in which the carbide exhibits significant reactivity, e.g., III,[3-5] and the conversion of the η^2-CO in II to the exposed carbide in III has been achieved.[6]

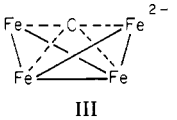

III

In this paper we explore further the structural consequences of electrophilic attack on these four-iron systems. We find that the carbide in III is attacked by the methyl carbocation, yielding a product containing a tetrahedral four-iron skeleton. Protonation of III has been previously shown to occur in the metal framework, leaving the four-iron butterfly intact.

The tetrahedral cluster $[Fe_4(CO)_{12}(\mu_3\text{-}CO)]^{2-}$ (I) contains a μ^3-CO bridging one face and three semibridging CO ligands between the iron atoms of this unique fact, V.[7] In contrast to the protonation reaction, which occurs on the iron framework and transforms the tetrahedron into a butterfly array (eq 1) alkylation occurs on the oxygen of the face-bridging CO and leaves the tetrahedral array of iron atoms intact. The sites of attack and structural rearrangements provide valuable insight into the reactivity patterns of metal carbonyl and carbide cluster compounds.[8]

Experimental Section

General Procedures. Inert atmosphere Schlenk and dry-box techniques were used in handling all of the iron cluster compounds. Solvents were rigorously dried and degassed prior to use. $[PPN]_2[Fe_4(CO)_{12}(\mu_3\text{-}CO)]$ was synthesized by modifications of the procedure of Hieber and Werner for the synthesis of other salts of this polynuclear iron–carbonyl anion[9,10] (PPN = bis(triphenylphosphine)nitrogen cation). $[PPN]_2[Fe_4(CO)_{12}C]$ was prepared by addition of methanolic KOH to a methanol solution of $HFe_4(CO)_{12}(CH)$,[4] addition of a slight excess of [PPN]Cl in methanol, and collection of the precipitate, which was washed with methanol. The infrared spectrum of this compound in CH_2Cl_2 solution agreed with the published infrared spectrum for the anion.[4] Triflic acid (HSO_3CF_3) and methyl fluorosulfate (CH_3SO_3F) were distilled in an all-glass apparatus and stored in containers in which they were exposed to glass and Teflon surfaces only.[11]

(1) (a) Oklahoma State University. (b) Northwestern University.
(2) Monassero, M.; Sansoni, M.; Longoni, G. *J. Chem. Soc., Chem. Commun.* **1976**, 919.
(3) Bradley, J. S.; Ansell, G. B.; Hill, E. W. *J. Am. Chem. Soc.* **1979**, *101*, 7417. Bradley, J. S.; Ansell, G. B.; Leonowicz, M. E.; Hill, E. W. *Ibid.* **1981**, *103*, 4968.
(4) Tachikawa, M.; Muetterties, E. L. *J. Am. Chem. Soc.* **1980**, *102*, 4541.
(5) Davis, J. H.; Beno, M. A.; Williams, J. M.; Zummie, J.; Tachikawa, M.; Muetterties, E. L. *Proc. Natl. Acad. Sci.* **1981**, *78*, 668.
(6) Holt, E. M.; Whitmire, K. H.; Shriver, D. F. *J. Organomet. Chem.* **1981**, *213*, 125.
(7) Dodens, R. J.; Dahl, L. F. *J. Am. Chem. Soc.* **1966**, *88*, 4847.
(8) A preliminary report has appeared: Holt, E. M.; Whitmire, K.; Shriver, D. F. *J. Chem. Soc., Chem. Commun.* **1980**, 778.
(9) Hieber, W.; Werner, R. *Chem. Ber.* **1957**, *90*, 286.
(10) Whitmire, K.; Ross, J.; Copper, C. B., III; Shriver, D. F. *Inorg. Synth.* **1982**, *21*, 66.

0002-7863/82/1504-5621$01.25/0

Table I. Crystal Data

	IV	V
M_r	1125.16	1141.1
space group	$P1$	$P\bar{1}$
systematic absences	none	none
a, Å	16.492 (5)	11.131 (3)
b, Å	17.648 (5)	14.064 (13)
c, Å	18.859 (7)	15.790 (4)
α, deg	62.93 (3)	93.27 (8)
β, deg	89.79 (3)	95.07 (3)
γ, deg	89.62 (3)	91.66 (4)
V, Å^3	4887.49	2456.8
Z	4	2
$F(000)$	2279	1156
D_{calcd}, g cm^{-3}	1.529	1.542
μ(Mo Kα), cm^{-1}	12.89	13.24
D_{obsd} ($I > 3\sigma(I)$)	7110	6327
R, %	5.5	4.6

Unless otherwise noted, ^{13}C NMR species were obtained on Varian CFT-20 or JEOL FX-90Q spectrometers, infrared spectra were determined on a Perkin-Elmer 399 or 283 spectrometer, and mass spectra were determined on a Hewlett-Packard 5985 quadrupole spectrometer using 15–20-eV electron impact.

Preparation of [PPN][$Fe_4(CO)_{12}(\mu_3$-$COCH_3)$]. To 1.0 g of $[PPN]_2[Fe_4(CO)_{13}]$ in 5 mL of CH_2Cl_2 was added, while stirring, 0.1 mL of CH_3SO_3F. The solution was allowed to react for about 1 h, at which time the CH_2Cl_2 was removed under vacuum. The product was dissolved in 15 mL of diethyl ether, and the white precipitate was removed by filtration. Hexane (30–60 mL) was then layered on the ether filtrate, and a crystalline product was allowed to precipitate slowly. The solvent was removed by filtration and the product dried under vacuum. Anal. Calcd for $C_{50}H_{33}NFe_4O_{13}P_2$: C, 52.63; H, 2.91; N, 1.23. Found: C, 51.80; H, 2.75; N, 1.36. IR ν_{CO} (Fluorolube) 2045 m, 1970 vs, 1933 w, 1920 w, 1912 w, 1864 m cm^{-1}; (CH_2Cl_2 solution) 1980 vs cm^{-1}. ^1H NMR (CD_2Cl_2) δ 7.58 (multiplet, PPN^+), 4.49 (CH_3). Small dark purple single crystals suitable for X-ray analysis were obtained by slow cooling of a concentrated methanol solution of the product.

Preparation of [PPN][$Fe_4(CO)_{12}(\mu_3$-$CCH_3)$]. To 2.5 g of $[PPN]_2[Fe_4(CO)_{12}C]$ in 30 mL of CH_2Cl_2 was added 0.3 mL of CH_3SO_3F. After about 1 h, the solvent was removed under vacuum, leaving a dark red-black solid that was dissolved in diethyl ether. This solution was filtered, leaving a grey-white solid. Hexane addition to the ether solution caused the precipitation of a red-black crystalline product (yield = 1.2 g, 72%). Small crystals suitable for single-crystal X-ray analysis were obtained by slow cooling of a concentrated methanol solution of the product. The dark red-brown product was somewhat soluble in toluene as well as in CH_2Cl_2, methanol, and diethyl ether. Anal. Calcd for $C_{50}H_{33}NFe_4O_{12}P_2$: C, 53.38; H, 2.96; N, 1.24; Fe, 19.85. Found: C, 52.45; H, 3.01; N, 1.49; Fe, 18.42. IR ν_{CO} (CH_2Cl_2) 2041 w, 1993 w sh, 1980 vs, 1935 m sh cm^{-1}. ^1H NMR δ 7.5 (PPN^+ cation), 4.18 (CH_3).

X-ray Structure Determination. Single crystals of $[PPN][Fe_4(CO)_{12}(\mu_3$-$CCH_3]$ and $[PPN][Fe_4(CO)_{12}(\mu_3$-$COCH_3)$ were sealed in capillaries and mounted on automated Nicolet diffractometers. Unit cell dimensions were determined during normal alignment procedures. Data were collected at room temperature by using a θ–2θ scan technique, variable scan range, and Mo Kα radiation. Observed data ($I > 3\sigma(I)$) were corrected for Lorentz, polarization, and background effects and used for solution of the structures (combined direct methods and Patterson techniques). Owing to the large number of parameters, block-matrx least-squares refinement was performed on the scale factor, positional parameters, and anisotropic thermal parameters for all non-hydrogen atoms. Unit weights were used throughout. The crystal data are summarized in Table I.

Results and Discussion

Crystal Structures. The clusters $[Fe_4(CO)_{12}(\mu_3$-$CCH_3)]^-$ (IV) and $[Fe_4(CO)_{12}(\mu_3$-$COCH_3)]^-$ (V) show a similar tetrahedral arrangement of the four iron atoms bridged symmetrically on one face by a μ_3 group (Figures 1 and 2). Each iron is further coordinated to three carbonyl carbon atoms, and the two anionic clusters display 60-electron frameworks. A PPN cation balances the negative charge in the cell. The average iron–iron distances [2.554 (3) Å, IV, and 2.581 (2) Å, V] are comparable to the 2.54 Å observed in $Fe_4(CO)_9(\mu$-$CO)_3(\mu_3$-$CO)^{2-}$, which is also a 60-electron 4-iron cluster of tetrahedral structure.[7] Similarly, IV and V exhibit shorter Fe–Fe distances on the bridged face of the tetrahedron [2.529 (3) Å, IV, and 2.555 (2) Å, V] than they do to the apical iron atom [2.576 (2) Å, IV, and 2.608 (2) Å, V], as does $Fe_4(CO)_9(\mu$-$CO)_3(\mu_3$-$CO)^{2-}$ (2.50 and 2.58 Å, respectively).[7] Comparisons may be made of the relative strength of the bonding of the μ_3 species in the three tetrahedral clusters. Average Fe–C distances to the μ_3 carbon [μ_3-CO, 2.00 Å; μ_3-$COCH_3$, 1.932 (8) Å; μ_3-CCH_3, 1.91 (1) Å] show bond distances decreasing with increasing electron-accepting character of the μ_3 species (CO vs. $COCH_3^+$ vs. CCH_3^+). The fourth bond to the μ_3 species is nearly perpendicular to the triangular face of the cluster in all three cases. Thus Fe–C1–C2 and Fe–C3–C4 angles show a narrow range [128.9 (9)–132.3 (9)°] in IV, as doe Fe–μ_3–C–O angles [128.2 (6)–132.5 (6)°] in V and the Fe–μ_3–C–O angles [132 (2)–133 (2)°] in I. In both structures reported here, the PPN catin displays the common bent geometry with normal distances and angles.

One other iron cluster containing a face-bridging ethyne has been reported, $H_3Fe_3(CO)_9(\mu_3$-$CCH_3)$,[12] and it is of interest to compare spectral and structural parameters for this three-iron cluster with those found in the present research for the four-iron cluster. The ^1H NMR resonance for the methyl group in $H_3Fe_3(CO)_9(\mu_3$-$CCH_3)$ occurs at 4.33 ppm. The present four-iron cluster displays a similar low-field methyl resonance, 4.18 ppm. The average Fe–C distance to the ethyne carbon is ca. 0.04 Å longer in the trinuclear system, and the C–CH_3 distance is shorter by ca. 0.1 Å, indicating weaker ethyne–metal interaction in the three-iron cluster. If we view the buildup of each cluster from

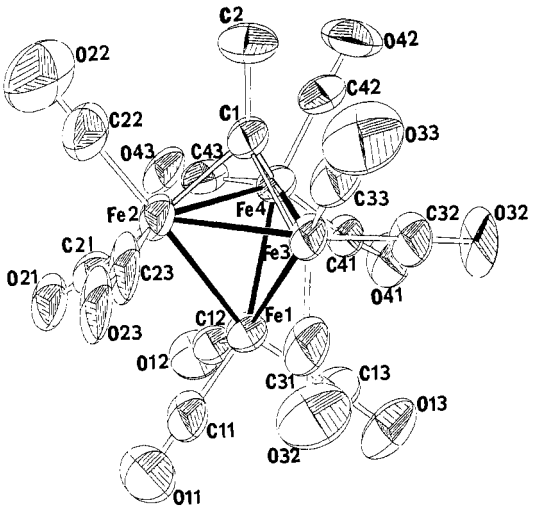

Figure 1. ORTEP diagram of the structure of $[Fe_4(CO)_{12}(CCH_3)]^-$ (IV).

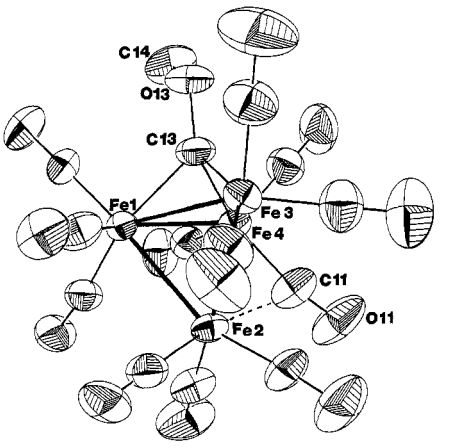

Figure 2. ORTEP diagram of the structure of $[Fe_4(CO)_{12}(COCH_3)]^-$ (V).

(11) Shriver, D. F. "The Manipulation in Air-Sensitive Compounds"; McGraw-Hill: New York, 1969; p 104.

(12) Wong, K. S.; Fehlner, T. P. *J. Am. Chem. Soc.* **1981**, *103*, 966.

Table II. Bond Distances (Å) and Angles (Deg) for $Fe_4C_{50}H_{33}NO_{12}P_2$

Fe1–Fe2	2.577 (2)	Fe5–Fe6	2.576 (3)
Fe1–Fe3	2.575 (2)	Fe5–Fe7	2.592 (3)
Fe1–Fe4	2.576 (3)	Fe5–Fe8	2.570 (3)
Fe2–Fe3	2.529 (3)	Fe6–Fe7	2.512 (3)
Fe2–Fe4	2.530 (3)	Fe6–Fe8	2.514 (3)
Fe3–Fe4	2.529 (3)	Fe7–Fe8	2.526 (3)
Fe1–C11	1.76 (1)	Fe5–C51	1.77 (2)
Fe1–C12	1.76 (1)	Fe5–C52	1.71 (1)
Fe1–C13	1.74 (1)	Fe5–C53	1.75 (2)
Fe2–C21	1.76 (1)	Fe6–C61	1.71 (2)
Fe2–C22	1.71 (1)	Fe6–C62	1.73 (2)
Fe2–C23	1.73 (2)	Fe6–C63	1.75 (1)
Fe3–C31	1.77 (2)	Fe7–C71	1.71 (1)
Fe3–C32	1.72 (2)	Fe7–C72	1.78 (2)
Fe3–C33	1.73 (2)	Fe7–C73	1.78 (2)
Fe4–C41	1.75 (1)	Fe8–C81	1.74 (1)
Fe4–C42	1.76 (2)	Fe8–C82	1.76 (2)
Fe4–C43	1.74 (2)	Fe8–C83	1.80 (1)
Fe2–C1	1.89 (1)	Fe6–C3	1.89 (1)
Fe3–C1	1.91 (1)	Fe7–C3	1.93 (2)
Fe4–C1	1.92 (1)	Fe8–C3	1.94 (1)
C1–C2	1.58 (1)	C3–C4	1.54 (2)
C11–O11	1.15 (2)	C51–O51	1.15 (2)
C12–O12	1.13 (2)	C52–O52	1.20 (1)
C13–O13	1.16 (2)	C53–O53	1.15 (3)
C24–O24	1.17 (1)	C61–O61	1.21 (2)
C22–O22	1.18 (2)	C62–O62	1.16 (2)
C23–O23	1.19 (2)	C63–O63	1.17 (2)
C31–O31	1.14 (2)	C71–O71	1.18 (1)
C32–O32	1.16 (2)	C72–O72	1.15 (2)
C33–O33	1.17 (2)	C73–O73	1.14 (2)
C41–O41	1.18 (2)	C81–O81	1.15 (2)
C42–O42	1.15 (2)	C82–O82	1.15 (2)
C43–O43	1.17 (2)	C83–O83	1.14 (1)
Fe5–C51–O51	179.4 (14)	Fe1–C11–O11	179.2 (12)
Fe5–C52–O52	178.2 (14)	Fe1–C12–O12	178.7 (13)
Fe5–C53–O53	173.1 (16)	Fe1–C13–O13	176.1 (10)
Fe6–C61–O61	170.1 (13)	Fe2–C21–O21	171.2 (10)
Fe6–C62–O62	176.9 (11)	Fe2–C22–O22	178.9 (13)
Fe6–C63–O63	174.8 (12)	Fe2–C23–O23	175.8 (12)
Fe7–C71–O71	178.0 (11)	Fe3–C31–O31	174.3 (12)
Fe7–C72–O72	172.7 (11)	Fe3–C32–O32	174.7 (16)
Fe7–C73–O73	177.0 (13)	Fe3–C33–O33	176.4 (14)
Fe8–C81–O81	176.4 (15)	Fe4–C41–O41	173.4 (12)
Fe8–C82–O82	177.0 (13)	Fe4–C42–O42	178.6 (13)
Fe8–C83–O83	171.7 (16)	Fe4–C43–O43	176.6 (14)

a negative metal–cluster moiety and a carbocation ligand, CCH_3^+, the difference in bonding can be attributed to the availability of greater electron density in the four-iron system, owing to both the larger net negative charge of the four-iron cluster and to the additional electron density available from the fourth iron atom.

The four-iron clusters, I, IV, and V, differ widely in configuration of their non-μ_3 carbonyl ligands. Whereas I displays three semibridging carbonyls spanning the edges of the face-bridged iron triangle, IV shows only terminal carbonyl bonding, and V has eleven terminal carbonyl groups and only one semibridging carbonyl [Fe1–C1, 1.968 (8) Å; Fe2–C11, 2.458 (9) Å; Fe1–C11–O11, 164.6 (8)°], which spans the apical iron atom and an iron atom of the bridged face. It might be noted that each of the two independent clusters of the asymmetric unit of structure IV has one carbonyl group with Fe–C–O angle close to 170° bonded to an iron of the μ_3 bridged face (C21) and C61), which is closer to the apical iron atom (2.68 and 2.59 Å, respectively) than is normally observed for terminal carbonyl groups but not close enough to be semibridging under normal criteria (2.43–2.46 Å bridging distance). The lengthening of the Fe–C bond normally associated with μ carbonyl bonding is similarly not observed. Fe–C distances for terminal carbonyl groups, which average 1.75 Å for IV and 1.78 Å for V are normal, as are the average C–O distances (1.16 Å, IV, and 1.145 Å, V). Other bond distances and angles are given for IV in Table II and for V in Table III. Positional parameters for these two compounds are given in Tables IV and V.

Table III. Distances (Å) and Bond Angles (Deg) for $Fe_4C_{50}O_{13}H_{33}P_2N$

Fe1–Fe2	2.614 (2)	Fe1–C13	1.968 (8)
Fe1–Fe3	2.550 (2)	Fe3–C13	1.924 (8)
Fe1–Fe4	2.559 (3)	Fe4–C13	1.903 (8)
Fe2–Fe3	2.641 (2)	C13–O13	1.365 (9)
Fe2–Fe4	2.570 (2)	O13–C14	1.465 (10)
Fe3–Fe4	2.557 (2)	P1–N1	1.585 (6)
Fe1–C1	1.793 (8)	P2–N1	1.593 (5)
Fe1–C2	1.792 (8)	C1–O1	1.15 (1)
Fe1–C3	1.771 (9)	C2–O2	1.13 (1)
Fe2–C11	2.458 (9)	C3–O3	1.15 (1)
Fe2–C4	1.782 (10)	C4–O4	1.14 (1)
Fe2–C5	1.779 (9)	C5–O5	1.15 (1)
Fe2–C6	1.781 (9)	C6–O6	1.14 (1)
Fe3–C7	1.784 (8)	C7–O7	1.16 (1)
Fe3–C8	1.792 (9)	C8–O8	1.13 (1)
Fe3–C9	1.772 (10)	C9–O9	1.15 (1)
Fe4–C10	1.769 (9)	C10–O10	1.15 (1)
Fe4–C11	1.795 (10)	C11–O11	1.15 (1)
Fe4–C12	1.766 (9)	C12–O12	1.14 (1)
Fe1–C1–O1	173.8 (8)	Fe4–Fe3–Fe1	60.15 (6)
Fe2–C2–O2	176.3 (8)	Fe3–Fe4–Fe1	59.79 (4)
Fe2–C3–O3	177.0 (8)	Fe3–Fe1–Fe4	60.06 (6)
Fe2–C4–O4	179 (1)	Fe3–Fe2–Fe4	58.76 (4)
Fe2–C5–O5	176.3 (8)	Fe3–Fe2–Fe1	58.06 (4)
Fe2–C6–O6	177.4 (8)	Fe4–Fe2–Fe1	59.16 (6)
Fe3–C7–O7	175 (1)	Fe3–C13–Fe4	83.8 (3)
Fe3–C8–O8	179 (2)	Fe4–C13–Fe1	82.8 (3)
Fe3–C9–O9	177.3 (10)	Fe1–C13–Fe3	81.9 (3)
Fe4–C10–O10	176.3 (9)	P1–N1–P2	141.4 (4)
Fe4–C11–O11	164.6 (8)	C13–O13–C14	117.3 (6)
Fe4–C12–O12	178.6 (9)		

Chemistry and Bonding. The foregoing structural data demonstrate that the alkylation of $[Fe_4(CO)_{12}C]^{2-}$ (III) by CH_3SO_3F, which proceeds rapidly, leads to a reorganization of the four-iron butterfly array to a tetrahedron (IV eq 2. The ^{13}C NMR at −90

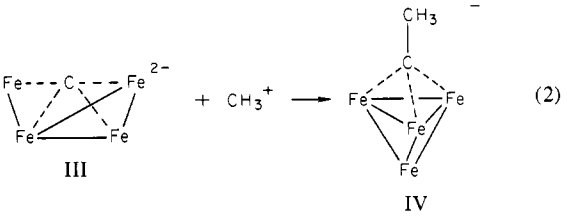

°C of this product, which was enriched only at the iron-bound carbons, displays a simple intensity pattern: 1:9:3. The peak of intensity 1 occurs at low field, 357.0 ppm, which is characteristic of a metal-bound carbide, whereas the other features are at 217.8 and 216.4 ppm, which is the characteristic region of terminal carbonyls. This solution spectrum is fully consistent with the X-ray crystal structure if it is assumed that the nine CO ligands around the iron triangle in the unique base of the tetrahedron (iron atoms 2, 3, and 4 in Figure 1) are equivalent on the NMR time scale, as are the three CO ligands on the unique vertex, Fe1. This type of equivalence is often seen for the CO ligands in clusters of this sort, and mechanisms involving local rotation of the $(CO)_3$ arrays or by bridge–terminal CO interchange are frequently invoked. Likewise, the infrared spectum in solution is consistent with the crystal structure in that it shows a simple pattern in the terminal CO region and no bridging-CO stretching modes. Judging from a recent report, structure of the product of reaction 2 may be dependent on the nature of the alkylating agent. Thus Tachikawa and Muetterties describe preliminary results on the alkylation of I by methyl iodide to yield a different product, displaying an infrared band characteristic of an acetyl oxygen.[5]

The structural rearrangement shown in eq 2 is readily understood by using the cluster valence electron counting schemes recently espoused by Wade, Mingos, and Lauher.[13–15] Lauher,

(13) Wade, K. *Adv. Inorg. Chem. Radiochem.* **1976**, *18*, 67.
(14) Mingos, D. M. P. *Nature (London), Phys. Sci.* **1972**, *236*, 99.

Table IV. Positional Parameters for $Fe_4C_{50}H_{33}NO_{12}P_2$

atom	x	y	z	atom	x	y	z
Fe1	0.7280 (1)	0.6228 (1)	0.6511 (1)	C121	0.2837 (7)	0.2926 (8)	0.8709 (6)
Fe2	0.6534 (1)	0.4925 (1)	0.7574 (1)	C122	0.2328 (9)	0.2269 (8)	0.8733 (7)
Fe3	0.8041 (1)	0.4829 (1)	0.7370 (1)	C123	0.2714 (10)	0.1494 (9)	0.8816 (8)
Fe4	0.7520 (1)	0.5726 (1)	0.8008 (1)	C124	0.3570 (12)	0.1459 (11)	0.8870 (9)
C11	0.6816 (7)	0.6125 (7)	0.5720 (7)	C125	0.4032 (10)	0.2076 (12)	0.8861 (8)
O11	0.6506 (6)	0.6065 (6)	0.5199 (5)	C126	0.3668 (8)	0.2857 (9)	0.8763 (7)
C12	0.6756 (8)	0.7158 (7)	0.6382 (7)	C131	0.1498 (6)	0.3660 (6)	0.9210 (6)
O12	0.6433 (6)	0.7766 (5)	0.6287 (5)	C132	0.1584 (8)	0.2993 (8)	1.0006 (7)
C13	0.8134 (8)	0.6761 (8)	0.5970 (7)	C133	0.0936 (10)	0.2857 (10)	1.0540 (9)
O13	0.8675 (6)	0.7144 (6)	0.5574 (6)	C134	0.0230 (10)	0.3335 (12)	1.0288 (11)
C21	0.5781 (7)	0.5690 (7)	0.7078 (7)	C135	0.0159 (9)	0.3974 (9)	0.9513 (10)
O21	0.5206 (5)	0.6119 (6)	0.6804 (6)	C136	0.0796 (7)	0.4124 (7)	0.8972 (7)
C22	0.5898 (8)	0.4299 (9)	0.8330 (9)	C211	0.1370 (6)	0.5434 (6)	0.6173 (6)
O22	0.5472 (7)	0.3862 (8)	0.8858 (8)	C212	0.1374 (8)	0.6134 (7)	0.6331 (7)
C23	0.6481 (8)	0.4334 (8)	0.7055 (9)	C213	0.0932 (9)	0.6880 (8)	0.5801 (9)
O23	0.6396 (6)	0.3913 (7)	0.6718 (7)	C214	0.0520 (8)	0.6876 (8)	0.5158 (8)
C31	0.8107 (9)	0.4937 (9)	0.6391 (9)	C215	0.0512 (9)	0.6179 (8)	0.5019 (8)
O31	0.8194 (8)	0.4951 (7)	0.5784 (7)	C216	0.0933 (8)	0.5443 (8)	0.5536 (7)
C32	0.8958 (9)	0.5280 (8)	0.7384 (8)	C221	0.1522 (7)	0.3623 (7)	0.6777 (7)
O32	0.9603 (6)	0.5538 (7)	0.7378 (6)	C222	0.1842 (8)	0.3226 (7)	0.6346 (7)
C33	0.8415 (9)	0.3796 (10)	0.7802 (9)	C223	0.1439 (9)	0.2498 (8)	0.6371 (8)
O33	0.8708 (8)	0.3114 (7)	0.8086 (8)	C224	0.0727 (9)	0.2203 (8)	0.6813 (8)
C41	0.8138 (8)	0.6626 (8)	0.7550 (8)	C225	0.0405 (9)	0.2625 (9)	0.7221 (8)
O41	0.8579 (6)	0.7212 (6)	0.7317 (6)	C226	0.0800 (8)	0.3330 (8)	0.7210 (8)
C42	0.7978 (9)	0.5418 (9)	0.8939 (8)	C231	0.2959 (6)	0.4680 (7)	0.6364 (6)
O42	0.8280 (7)	0.5199 (7)	0.9552 (6)	C232	0.3544 (7)	0.4038 (7)	0.6738 (6)
C43	0.6654 (9)	0.6201 (9)	0.8160 (7)	C233	0.4346 (8)	0.4176 (9)	0.6468 (8)
O43	0.6086 (6)	0.6533 (6)	0.8277 (6)	C234	0.4566 (8)	0.4957 (10)	0.5851 (9)
C1	0.7405 (7)	0.4535 (7)	0.8308 (7)	C235	0.3999 (9)	0.5586 (9)	0.5466 (8)
C2	0.7482 (9)	0.3740 (8)	0.9152 (7)	C236	0.3166 (8)	0.5453 (7)	0.5722 (7)
Fe5	0.2961 (1)	−0.1337 (1)	0.2429 (1)	N2	0.7851 (6)	0.0414 (5)	0.2630 (5)
Fe6	0.2042 (1)	−0.0324 (1)	0.2718 (1)	P3	0.7468 (2)	0.0083 (2)	0.3484 (2)
Fe7	0.3082 (1)	0.0303 (1)	0.1629 (1)	P4	0.7875 (2)	0.1248 (2)	0.1804 (2)
Fe8	0.3523 (1)	−0.0438 (1)	0.3070 (1)	C311	0.6794 (7)	−0.0772 (6)	0.3664 (6)
C51	0.3920 (9)	−0.1790 (9)	0.2429 (8)	C312	0.6281 (8)	−0.1099 (8)	0.4330 (7)
O51	0.4541 (7)	−0.2093 (7)	0.2430 (6)	C313	0.5770 (9)	−0.1799 (9)	0.4458 (8)
C52	0.2541 (8)	−0.2258 (8)	0.3132 (8)	C314	0.5769 (9)	−0.2140 (8)	0.3927 (9)
O52	0.2226 (6)	−0.2892 (6)	0.3623 (6)	C315	0.6278 (8)	−0.1809 (8)	0.3268 (9)
C53	0.2630 (9)	−0.1419 (11)	0.1586 (9)	C316	0.6802 (7)	−0.1126 (7)	0.3133 (7)
O53	0.2449 (8)	−0.1553 (8)	0.1065 (7)	C321	0.8289 (7)	−0.0331 (6)	0.4202 (6)
C61	0.1454 (9)	−0.0896 (9)	0.2392 (8)	C322	0.9046 (7)	−0.0429 (7)	0.3934 (7)
O61	0.0953 (6)	−0.1202 (6)	0.2131 (7)	C323	0.9683 (8)	−0.0774 (8)	0.4498 (8)
C62	0.1287 (8)	0.0410 (9)	0.2587 (7)	C324	0.9541 (9)	−0.1013 (8)	0.5300 (8)
O62	0.0772 (6)	0.0886 (7)	0.2536 (6)	C325	0.8774 (10)	−0.0926 (8)	0.5563 (8)
C63	0.1920 (8)	−0.0927 (8)	0.3749 (7)	C326	0.8129 (8)	−0.0577 (7)	0.5006 (6)
O63	0.1782 (6)	−0.1300 (6)	0.4432 (5)	C331	0.6919 (7)	0.0861 (6)	0.3669 (6)
C71	0.3335 (7)	0.1359 (8)	0.1140 (7)	C332	0.7359 (8)	0.1388 (7)	0.3891 (7)
O71	0.3485 (6)	0.2091 (5)	0.0801 (5)	C333	0.6946 (9)	0.2048 (8)	0.3978 (8)
C72	0.3831 (9)	−0.0054 (8)	0.1165 (8)	C334	0.6106 (10)	0.2161 (9)	0.3838 (8)
O72	0.4326 (8)	−0.0196 (7)	0.0807 (6)	C335	0.5686 (9)	0.1617 (10)	0.3615 (8)
C73	0.2252 (9)	0.0408 (10)	0.0991 (9)	C336	0.6088 (8)	0.0957 (8)	0.3526 (7)
O73	0.1738 (7)	0.0506 (8)	0.0559 (6)	C411	0.8582 (7)	0.1042 (7)	0.1193 (6)
C81	0.4488 (8)	−0.0219 (8)	0.2644 (8)	C412	0.8965 (10)	0.0257 (9)	0.1459 (8)
O81	0.5140 (6)	−0.0071 (6)	0.2397 (6)	C413	0.9578 (12)	0.0168 (13)	0.0972 (10)
C82	0.3716 (9)	−0.0073 (8)	0.3777 (8)	C414	0.9784 (10)	0.0865 (12)	0.0234 (9)
O82	0.3876 (7)	0.0173 (7)	0.4226 (6)	C415	0.9360 (10)	0.1618 (10)	−0.0046 (9)
C83	0.3618 (8)	−0.1533 (9)	0.3809 (8)	C416	0.8777 (8)	0.1708 (8)	0.0454 (8)
O83	0.3716 (6)	−0.2191 (6)	0.4337 (6)	C421	0.8290 (6)	0.2146 (6)	0.1885 (6)
C3	0.2818 (7)	0.0538 (7)	0.2511 (7)	C422	0.8007 (8)	0.2978 (8)	0.1408 (7)
C4	0.2782 (9)	0.1379 (7)	0.2570 (8)	C423	0.8416 (8)	0.3658 (8)	0.1479 (7)
N1	0.1984 (5)	0.4454 (5)	0.7661 (5)	C424	0.9077 (8)	0.3491 (8)	0.1984 (8)
P1	0.2324 (2)	0.3912 (2)	0.8525 (2)	C425	0.9343 (8)	0.2650 (9)	0.2446 (7)
P2	0.1972 (2)	0.4528 (2)	0.6794 (2)	C426	0.8949 (7)	0.1970 (8)	0.2394 (7)
C111	0.3031 (6)	0.4539 (7)	0.8744 (6)	C431	0.6920 (7)	0.1538 (7)	0.1292 (6)
C112	0.3267 (8)	0.4321 (8)	0.9532 (7)	C432	0.6336 (8)	0.1956 (8)	0.1519 (7)
C113	0.3802 (9)	0.4839 (10)	0.9675 (8)	C433	0.5562 (8)	0.2136 (8)	0.1130 (8)
C114	0.4122 (9)	0.5573 (9)	0.9058 (9)	C434	0.5424 (9)	0.1889 (10)	0.0538 (8)
C115	0.3899 (9)	0.5776 (8)	0.8284 (8)	C435	0.6015 (10)	0.1453 (11)	0.0334 (9)
C116	0.3343 (7)	0.5271 (8)	0.8118 (7)	C436	0.6767 (8)	0.1267 (9)	0.0702 (8)

in particular, has considered the electron count appropriate to the various geometries of M_4 species.[15] A good HOMO–LUMO gap is calculated for a tetrahedral array having 60 cluster valence electrons and for a butterfly having 62 CVE. The four-iron butterfly carbide has the expected 62 CVE if the carbide is reckoned to be a four-electron donor (as indicated by extended Hückel calculations in an accompanying paper;[16] all of the carbide

(15) Lauher, J. W. *J. Am. Chem. Soc.* **1978**, *100*, 5305.

(16) Kolis, J. W.; Basolo, F.; Shriver, D. F. *J. Am. Chem. Soc.*, following paper in this issue.

Table V. Positional Parameters for $Fe_4C_{50}O_{13}H_{33}P_2N$

atom	x	y	z	atom	x	y	z
Fe1	0.3375 (1)	0.2319 (1)	0.2337 (1)	C112	0.3214 (6)	0.9656 (5)	0.5043 (4)
Fe2	0.2049 (1)	0.3512 (1)	0.1490 (1)	C113	0.3610 (7)	1.0484 (6)	0.5524 (5)
Fe3	0.4427 (1)	0.3574 (1)	0.1532 (1)	C114	0.2973 (7)	1.1321 (6)	0.5434 (5)
Fe4	0.3372 (1)	0.4077 (1)	0.2852 (1)	C115	0.1920 (8)	1.1321 (6)	0.4877 (5)
C1	0.1868 (7)	0.1973 (6)	0.2537 (5)	C116	0.1508 (7)	1.0476 (6)	0.4402 (5)
C2	0.4072 (7)	0.1552 (6)	0.3090 (6)	C121	0.2976 (6)	0.8326 (5)	0.3226 (4)
C3	0.3601 (8)	0.1510 (7)	0.1469 (5)	C122	0.3763 (6)	0.7589 (6)	0.3407 (5)
C4	0.0616 (9)	0.3621 (7)	0.1903 (6)	C123	0.4737 (8)	0.7457 (6)	0.2908 (6)
C5	0.1587 (7)	0.2512 (6)	0.0784 (6)	C124	0.4922 (8)	0.8046 (7)	0.2248 (6)
C6	0.1822 (8)	0.4375 (6)	0.0715 (5)	C125	0.4156 (8)	0.8801 (7)	0.2091 (6)
C7	0.4011 (8)	0.3116 (7)	0.0466 (6)	C126	0.3180 (7)	0.8945 (6)	0.2578 (6)
C8	0.6002 (8)	0.3389 (7)	0.1462 (6)	C131	0.1484 (6)	0.7653 (5)	0.4545 (4)
C9	0.4495 (9)	0.4801 (7)	0.1331 (6)	C132	0.1238 (6)	0.7881 (6)	0.5382 (5)
C10	0.2528 (8)	0.3741 (6)	0.3692 (6)	C133	0.1001 (8)	0.7157 (6)	0.5928 (6)
C11	0.2442 (9)	0.4979 (7)	0.2407 (6)	C134	0.0993 (8)	0.6220 (6)	0.5623 (6)
C12	0.4308 (8)	0.4908 (7)	0.3506 (6)	C135	0.1210 (7)	0.5972 (6)	0.4780 (6)
O1	0.0948 (5)	0.1685 (5)	0.2703 (4)	C136	0.1447 (7)	0.6698 (5)	0.4230 (6)
O2	0.4525 (6)	0.1037 (5)	0.3528 (4)	C211	−0.1080 (6)	0.7302 (4)	0.2505 (4)
O3	0.3769 (6)	0.0955 (5)	0.0928 (4)	C212	−0.1319 (6)	0.7049 (5)	0.3320 (4)
O4	−0.0305 (6)	0.3705 (7)	0.2158 (5)	C213	−0.1965 (7)	0.6194 (7)	0.3414 (5)
O5	0.1237 (6)	0.1895 (5)	0.0312 (4)	C214	−0.2396 (8)	0.5629 (7)	0.2705 (6)
O6	0.1640 (8)	0.4906 (5)	0.0206 (4)	C215	−0.2164 (9)	0.5885 (7)	0.1884 (6)
O7	0.3834 (7)	0.2803 (6)	−0.0233 (4)	C216	−0.1495 (8)	0.6721 (6)	0.1778 (5)
O8	0.6998 (6)	0.3276 (7)	0.1412 (6)	C221	0.0535 (6)	0.8381 (5)	0.1490 (4)
O9	0.4556 (8)	0.5585 (5)	0.1171 (6)	C222	0.0717 (6)	0.9219 (5)	0.1064 (4)
O10	0.2019 (6)	0.3558 (5)	0.4266 (4)	C223	0.1422 (8)	0.9203 (7)	0.0376 (6)
O11	0.1958 (8)	0.5675 (5)	0.2281 (4)	C224	0.1960 (9)	0.8354 (7)	0.0122 (6)
O12	0.4901 (7)	0.5439 (4)	0.3943 (4)	C225	0.1789 (10)	0.7529 (7)	0.0551 (7)
C13	0.4683 (6)	0.3263 (6)	0.2704 (5)	C226	0.1072 (8)	0.7533 (6)	0.1246 (5)
O13	0.5752 (4)	0.3157 (4)	0.3177 (4)	C231	−0.1465 (6)	0.9299 (5)	0.2217 (4)
C14	0.5725 (9)	0.3154 (8)	0.4103 (5)	C232	−0.2248 (6)	0.9168 (6)	0.1476 (5)
P1	0.1697 (2)	0.8593 (1)	0.3831 (1)	C233	−0.3151 (7)	0.9832 (6)	0.1304 (5)
P2	−0.0302 (2)	0.8448 (1)	0.2421 (1)	C234	−0.3259 (7)	1.0604 (6)	0.1869 (6)
N1	0.0491 (5)	0.8809 (4)	0.3274 (3)	C235	−0.2503 (9)	1.0732 (8)	0.2621 (7)
C111	0.2164 (6)	0.9656 (4)	0.4490 (4)	C236	−0.1593 (8)	1.0064 (6)	0.2802 (6)

2s and 2p orbitals contribute to the cluster molecular orbitals, so the carbon is correctly described as a four-electron source for the cluster valence electron count). When the CH_3^+ electrophile attaches to the carbide carbon in the butterfly, two electrons are removed from the pool of cluster framework electrons and localized into the C–CH_3 bond. The resulting 60 cluster valence electron count in the ethyne compound is appropriate for the observed tetrahedral geometry.[17]

As demonstrated by the X-ray structure data, the alkylation of $[Fe_4(CO)_{12}(\mu_3\text{-}CO)]^{2-}$ (**I**) occurs on the face-bridging carbonyl oxygen. This same structure persists in solution, as shown by the ^{13}C NMR spectra, which at room temperature display two features δ (CD_2Cl_2) 362.9 and 218.6 relative to Me_4Si in the ratio 1:12. The low-field resonance is assigned to the O-alkylated CO and the high-field resonance to the exchange-averaged signal of the remaining CO ligands. At low temperatures, the ^{13}C spectrum demonstrates that some of the fluctional character is removed: δ (CD_2Cl_2, −90 °C) 361.2 (singlet), 218.0 (singlet), and 213.8 (singlet) in the ratio 1:9:3. In contrast, the ^{13}C NMR of the parent, $[Fe_4(CO)_{12}(\mu\text{-}CO)]^{2-}$, shows a singlet to the lowest temperature studied, −100 °C, indicating high exchange mobility for all of the CO ligands. The ^1H NMR of $[Fe_4(CO)_{12}(\mu_3\text{-}COCH_3)]^-$ contains a single feature for the methyl group at δ (CD_2Cl_2) 4.49, in agreement with that for $[Fe_3(CO)_{10}(\mu_3\text{-}COCH_3)]^-$, δ (CD_2Cl_2) 4.33.[18,19]

The O-alkylation of a carbon monoxide ligand is the usual reaction of carbocation reagents with anionic cluster compounds containing bridging CO ligands.[16,18-23] The interaction with the face-bridging CO rather than the semibridging CO ligands is in

Scheme I

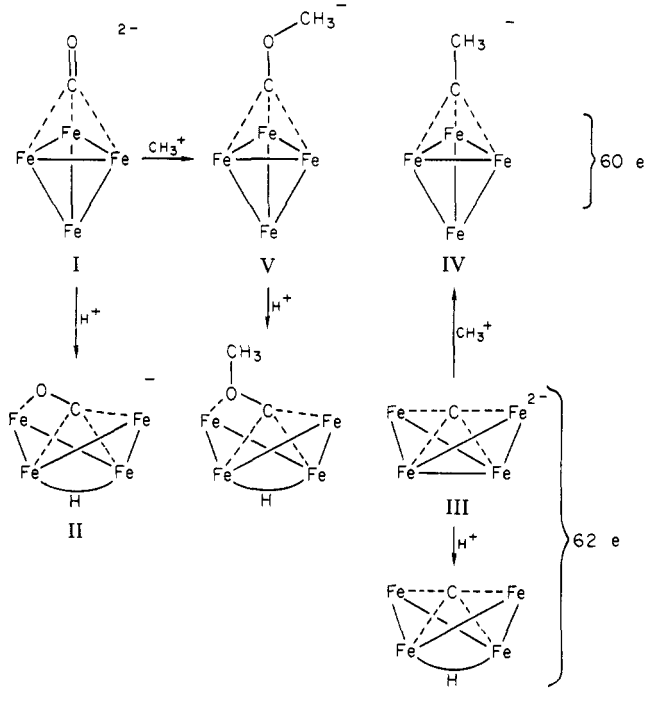

(17) In this discussion, the carbon atom is considered to be a ligand, but as a referee pointed out, there is a different way of viewing these structures in which the carbon atom is grouped with the metal atoms as a member of the cluster framework. In this scheme, IV would be a trigonal bipyramid with the carbon of the ethyne in an axial site, and the species $[Fe_4(CO)_{12}(CCO_2CH_3)]^-$ (ref 3) would be viewed as a trigonal bipyramid with a carbon atom in an equatorial site.

(18) Shriver, D. F.; Lehman, D.; Strope D. *J. Am. Chem. Soc.* **1975**, *97*, 1594.

(19) Hodali, H. A.; Shriver, D. F. *Inorg. Chem.* **1979**, *18*, 1236.

(20) Gavens, P. D.; Mays, M. J. *J. Organomet. Chem.* **1978**, *162*, 384.

(21) Dawson, P. A.; Johnson, B. F. G.; Lewis, J.; Rathby, P. R. *J. Chem. Soc., Chem. Commun.* **1980**, 781.

(22) Wong, W. K.; Wilkinson, G.; Galas, A. M. R.; Hursthouse, M. B.; Thornton-Pett, M. *J. Chem. Soc., Chem. Commun.* **1981**, 189.

(23) Keister, J. B. *J. Chem. Soc., Chem. Commun.* **1979**, 214.

keeping with the generalization that the order of basicity is terminal CO $\gg \mu_2$-CO $< \mu_3$-CO.[24] This alkylation does not change the electron count of the cluster valence electrons; however, it does bring about a redistribution of electron density away from existing metal framework MO's and into the alkylated CO. Evidence for this electron redistribution includes the shift of all terminal CO stretching absorption modes to higher frequencies, the lengthening of the μ_3-CO bond and shortening of the Fe–C bonds to the μ_3-CO, and a variety of physical evidence on other compounds containing an electrophile attached to a CO oxygen.[24-27] It is presumably this electron density shift that brings about a rearrangement of the semibridging CO ligands from the three semibridging COs in the parent anion, $[Fe_4(CO)_{12}(\mu_3\text{-CO})]^{2-}$ (I), to one in the alkylated product. From the chemical evidence cited above and a variety of physical data, bridging and semibridging CO ligands appear to withdraw more electron density than terminal CO; therefore, a semibridging disposition is favored for several CO ligands in the electron-rich cluster I, and the decrease in cluster electron density in the alkylated product V in electron-poor clusters causes a shift to terminal positions. One previous example of the shift of CO from bridging to terminal positions induced by an electrophile is known.[28]

(24) Alich, A.; Strope, D.; Shriver, D. F. *Inorg. Chem.*, **1972**, *11*, 2976.
(25) Shriver, D. F.; Alich, A. *Inorg. Chem.*, **1972**, *11*, 2984.
(26) Stimson, R. E.; Shriver, D. F. *Inorg. Chem.* **1980**, *19*, 1141.
(27) Hamilton, D. M.; Willis, W. S.; Stucky, G. D. *J. Am. Chem. Soc.* **1981**, *103*, 4255.
(28) Kristoff, J. S.; Shriver, D. F. *Inorg. Chem.* **1974**, *13*, 499.

The foregoing transformations are summarized along with some of the previously reported chemistry on these compounds in Scheme I. For simple tri- and tetranuclear dianionic iron carbonyl cluster compounds, O-alkylation occurs with strong carbocation reagents, whereas protonation occurs on the metal bonds. Presumably, the different site preference arises from the bulk of CH_3, which inhibits interaction with the metal centers. The protonation of the tetrahedral ions I and V has the remarkable effect of inducing a framework geometry change from tetrahedral to a butterfly array. One possible rationalization for this conversion is that the steric requirements of the H, while small, induce a more open structure.[2] This open (butterfly) structure requires two more cluster valence electrons, which is attained in the product by a shift of one CO into a dihapto configuration, converting it from a two-electron donor to a four-electron donor.

Acknowledgment. The portion of this research conducted at Northwestern University was supported by the NSF, through Grant CHE-7918010. E.M.H. thanks Dr. Chuck Campana of Nicolet-XRD for his assistance with the data collection on compound IV.

Registry No. $[PPN][Fe_4(CO)_{12}(\mu_3\text{-}COCH_3)]$, 79075-54-0; $[PPN][Fe_4(CO)_{12}(\mu_3\text{-}CCH_3)]$, 82865-65-4; $[PPN]_2[Fe_4(CO)_{12}(\mu_3\text{-CO})]$, 69665-30-1; $[PPN]_2[Fe_4(CO)_{12}C]$, 74792-05-5; $CH_3SO_3CF_3$, 333-27-7.

Supplementary Material Available: Positional and thermal parameters and observed and calculated structure factors (97 pages). Ordering information is given on any current masthead page.

Reactivity of Metal Carbide Clusters: Alkylation and Protonation of $[Fe_5(CO)_{14}C]^{2-}$

J. W. Kolis, F. Basolo, and D. F. Shriver*

Contribution from the Department of Chemistry, Northwestern University, Evanston, Illinois 60201. *Received January 19, 1982*

Abstract: The alkylation of $[Fe_5(CO)_{14}C]^{2-}$ was performed, and ^{13}C NMR indicates that alkylation occurs on a bridging carbonyl and not on the carbide. As judged by ^1H NMR, subsequent protonation occurs on the metal framework. This lack of reactivity of the carbide atom in the five-coordinate carbide cluster contrasts with reports of the protonation and alkylation of the four-coordinate carbide in Fe_4C clusters. Metal cluster carbides were investigated by extended Hückel calculations, which indicate a correlation between reactivity and the position of C-rich MO's relative to the HOMO and LUMO levels in the cluster. Model calculations on octahedral $(HFe)_6C$ and square-pyramidal $(HFe)_5C$ which lack reactivity at the carbide atom show a very large separation of molecular orbitals having significant carbon atomic orbital contributions. This MO separation is much smaller for the butterfly Fe_4C array and correlates well with the reactivity of this type of molecule. The MO calculations indicate that species of the type M_3C, having C_{3v} symmetry, are likely to be detectable.

The chemistry of metal carbide cluster compounds is an interesting and relatively unexplored area that may provide useful parallels with the chemistry of the surface carbides believed to be intermediates in the reduction of CO to hydrocarbons on Fe, Ru, and Ni.[1] In the present paper we explore the reactions of electrophiles, the proton and the methyl carbocation, toward the anionic iron carbonyl cluster $[Fe_5(CO)_{14}C]^{2-}$. This is one member of the series of anionic iron carbide clusters ranging from the octahedral $Fe_6(CO)_{16}C^{2-}$, which contains an enclosed octahedrally coordinated C;[2] to $[Fe_5(CO)_{14}C]^{2-}$, which has square-pyramidal coordination around the C atom;[3] to $[Fe_4(CO)_{12}C]^{2-}$, which has a four-coordinated C cradled between the wing tips of a butterfly

(1) (a) Tachikawa, M.; Muetterties, E. L. *Prog. Inorg. Chem.* **1981**, *28*, 203. (b) Muetterties, E. L.; Stein, J. *Chem. Rev.* **1979**, *79*, 479.
(2) Churchill, M. R.; Wormald, J.; Knight, J.; Mays, M. J. *J. Am. Chem. Soc.* **1971**, *93*, 3073.

(3) Tachikawa et al. [Tachikawa, M.; Geerts, R.; Muetterties, E. L. *J. Organomet. Chem.* **1981**, *213*, 11] present NMR evidence for the square pyramidal structure. The crystal structure of the neutral analogue, $Fe_5(CO)_{15}C$, shows the C atom projecting slightly from the basal Fe_4 plane away from the apical Fe; see ref 18. Even in $Fe_5(CO)_{15}C$, which presumably is more sterically congested than $[Fe_5(CO)_{14}C]^{2-}$, there is sufficient room around C for attack by H^+. From the crystallographic data and an estimated carbon van der Waals radius of 1.9 Å, we estimate a hole of radius in the range 0.6–0.9 Å available to a group attached to C in the neutral $Fe_5(CO)_{15}C$; this would not accommodate a hydrogen atom (van der Waals radius ca. 1.2). If the volume created by the loss of one CO were available on the basal face, the anion $[Fe_5(CO)_{14}C]^{2-}$ would have a radius in the range 4.0–4.3 Å available to a group attacking the carbide ion. This would be large enough to accommodate a CH_3 group (van der Waals radius 2.0).

0002-7863/82/1504-5626$01.25/0